Surgical Endoscopy (2019) 33:3200–3208
https://doi.org/10.1007/s00464-018-6603-4

Modular laser-based endoluminal ablation of the gastrointestinal tract: in vivo dose–effect evaluation and predictive numerical model

Giuseppe Quero[1] · Paola Saccomandi[1,2] · Jung-Myun Kwak[1,3] · Bernard Dallemagne[4] · Guido Costamagna[1] · Jacques Marescaux[1,4] · Didier Mutter[1,4,5] · Michele Diana[1,4,5]

Received: 10 June 2018 / Accepted: 13 November 2018 / Published online: 19 November 2018

Abstract

Background Endoscopic submucosal dissection allows for "en bloc" removal of early gastrointestinal neoplasms. However, it is technically demanding and time-consuming. Alternatives could rely on energy-based techniques. We aimed to evaluate a predictive numerical model of thermal damage to preoperatively define optimal laser settings allowing for a controlled ablation down to the submucosa, and the ability of confocal endomicroscopy to provide damage information.

Materials and methods A Nd:YAG laser was applied onto the gastric mucosa of 21 Wistar rats on 10 spots (total 210). Power settings ranging from 0.5 to 2.5W were applied during 1–12 s, with a consequent energy delivery varying from 0.5 to 30 J. Out of the 210 samples, a total of 1050 hematoxilin–eosin stained slides were obtained. To evaluate thermal injury, the ratio between the damage depth (DD) over the mucosa and the submucosa thickness (*T*) was calculated. Effective and safe ablation was considered for a DD/*T* ratio ≤ 1 (only mucosal and submucosal damage). Confocal endomicroscopy was performed before and after ablation. A numerical model, using human physical properties, was developed to predict thermal damage.

Results No full-thickness perforations were detected. On histology, the DD/*T* ratio at 0.5 J was 0.57 ± 0.21, significantly lower when compared to energies ranging from 15 J (a DD/T ratio $= 1.2 \pm 0.3$; $p < 0.001$) until 30 J (a DD/*T* ratio $= 1.33 \pm 0.31$; $p < 0.001$). Safe mucosal and submucosal ablations were achieved applying energy between 4 and 12 J, never impairing the muscularis propria. Confocal endomicroscopy showed a distorted gland architecture. The predicted damage depth demonstrated a significant positive linear correlation with the experimental data (Pearson's *r* 0.85; 95% CI 0.66–0.94).

Conclusions Low-power settings achieved effective and safe mucosal and submucosal ablation. The numerical model allowed for an accurate prediction of the ablated layers. Confocal endomicroscopy provided real-time thermal damage visualization. Further studies on larger animal models are required.

Keywords Laser ablation · Early gastrointestinal cancer · Confocal endomicroscopy · Preclinical study · Predictive numerical model

Endoscopic submucosal dissection (ESD) is an endoluminal surgical technique which allows for an *"en bloc"* removal of early gastrointestinal (GI) tumors, irrespective of lesion size. Additionally, ESD achieves a globally low R1 rate, ranging from 3.6 to 22.7% [1] and a lower recurrence rate when compared to endoscopic mucosal resection (EMR) [2, 3]. For these reasons, ESD is considered a valid alternative to the conventional surgical approach in the management of early GI tumors. However, ESD remains technically demanding with a significant risk of procedure-related early and late complications. In particular, a tumor diameter larger than 2 cm, the operator's experience, and the location of the lesions in difficult spots (cardia, duodenal bulb, and fundus) are recognized to be predisposing risk factors to

✉ Michele Diana
michele.diana@ircad.fr; michele.diana@ihu-strasbourg.eu

[1] IHU-Strasbourg, Institute of Image-Guided Surgery, Strasbourg, France

[2] Department of Mechanical Engineering, Politecnico di Milano, Milan, Italy

[3] Department of Surgery, Korea University College of Medicine, Seoul, Republic of Korea

[4] IRCAD, Research Institute Against Cancer of the Digestive System, 1, Place de l'Hôpital, 67091 Strasbourg, France

[5] Department of General, Digestive and Endocrine Surgery, University Hospital of Strasbourg, Strasbourg, France

adverse post-ESD events [4]. The rate of intraoperative perforations varies between 1.2 and 5.2% [5], while its delayed manifestation occurs in almost 0.5% of cases [6]. Similarly, intraoperative and delayed bleedings are reported in up to 7 [3] and 15.6% [5], respectively.

Alternative energy-based techniques have been proposed [7–12] to enable a safer and less demanding ablation.

Photodynamic therapy (PDT), based on a contactless application of a high-energy light source illuminating the lesion and the systemic administration of a photosensitizer [e.g., 5-delta-aminolevulinic acid (ALA)], has been used for Barrett's esophagus and early gastric cancer treatment [11, 12]. However, following a PDT treatment of tumors, a recurrence rate up to 18% has been reported [12]. Additionally, PDT is time-consuming, and the results are affected by breathing and peristaltic motions which lead to an inconstant targeting of the lesions.

Radiofrequency ablation (RFA) has been successfully applied for the treatment of Barrett's esophagus [9] and, more recently, for gastric dysplasia ablation [7]. However, currently available radiofrequency devices are set to perform superficial ablations, limited to the mucosa.

More recently, a Holmium:YAG (Ho:YAG) laser has been applied to treat intramucosal tumors, with positive results and no recurrence until 48.6 months of follow-up [10]. However, due to the low penetration depth (2140 nm wavelength), the application of this laser source could be limited to superficial lesions.

The Nd:YAG laser has a deeper tissue penetration (1064 nm wavelength), which would allow for an effective ablation of deeper layers, beyond the mucosa [13]. However, some disappointing results have been reported [14–18], including high perforation rates until 7%, in the treatment of esophageal cancer [19]. This could mainly be due to the lack of appropriate determination of optimal laser settings allowing for targeted layer ablation. Additionally, in order to effectively replace ESD, the energy source should be modular and patient-specific and directed toward ablation down to the submucosa, sparing deeper layers. To complete the set of requirements, which would allow for a larger adoption of energy-based endoscopic submucosal ablation, a real-time information providing a signature of a complete treatment would be ideal.

The primary aim of the present experimental study was to assess the possibility to achieve a controlled mucosal and submucosal ablation, without damaging the muscularis propria layer, by modulating Nd:YAG laser parameters, in terms of power and exposure time.

The secondary aim was to develop a predictive numerical model to simulate the thermal damage that would be induced on human tissues by specific laser settings.

Materials and methods

This experimental acute study was conducted in 21 male Wistar rats (mean weight 522 ± 47 g). Following the ethical principle of Reduction, animals were included at the end of a different experimental protocol, which received full approval from the Institutional Ethical Committee (Acronym HAMMER; Protocol No. 38.2015.01.073) and from the French Ministry of Superior Education and Research (Protocol No. APAFiS#2834). All animals used in the experimental laboratory were managed according to French laws for animal use and care and according to the directives of the European Community Council (2010/63/EU) with respect to the 3R principles (Replacement, Reduction, and Refinement). Anesthesia was maintained with 3% isoflurane. Animals were humanely killed at the end of the procedure.

Laser settings

A Nd:YAG laser system emitting near-infrared light (wavelength of 1064 nm) in a continuous way was used. The laser light is delivered from the tip (emitting surface of 0.28 mm^2) of an optical fiber applicator (300 µm-diameter), which is directly applied onto the treatment site.

Preliminary in vivo tests in six Wistar rats [20] led to the selection of adequate laser settings: at 3 W, independently of the duration of the application, and at 2.5 W applied for 13 s, a macroscopic full-thickness perforation of the stomach was detected, whereas no perforation was noted macroscopically for treatment at $P = 2.5$ W lasting 12 s. As a result, laser ablation treatments were performed at $P \leq 2.5$ W and $t \leq 12$ s, aiming to obtain ablation confined to mucosal and submucosal layers.

Five different power (P) values (0.5, 1.0, 1.5, 2.0, and 2.5 W) were chosen, and each was applied for seven different time (t) settings (1, 2, 4, 6, 8, 10, and 12 s). Each combination of P and t was repeated in six different animals, in order to consider the variation of gastric wall thickness among rats. Hence, six different types of laser damage were obtained for each P and t combinations.

Surgical procedure and real-time confocal endomicroscopy

Through a laparotomy approach, the stomach was exposed and opened longitudinally along the greater curvature, and the anterior and the posterior walls were exposed. Morphologically, the stomach of rats is divided into two regions: the forestomach, which corresponds to the upper portion and characterized by squamous epithelium, and the glandular stomach, which corresponds to the lower portion and

composed mainly of a cytological architecture similar to the human stomach. Due to this similarity, only the glandular stomach was considered for the study. Only the glandular stomach was considered for the study.

A total of 10 spots (5 on the anterior and 5 on the posterior wall) were randomly chosen for ablation (Total 210 spots).

For each selected treatment site, a histological real-time evaluation was obtained before laser ablation using a confocal endomicroscopy system (Cellvizio, Mauna Kea Technology, Paris, France). To obtain confocal images, 1 mL sodium fluorescein (Fluocyne 10%, SERB Laboratories) was injected into the spleen at the beginning of each surgical procedure. The probe used to image the gastric wall and to record a video was the Gastroflex UHD (240 µm-diameter FoV, 1 µm resolution, 55–65 µm confocal depth). The elapsed time between two consecutive endomicroscopies on the same treatment site was always less than 1 min.

The applicator tip of the laser was then applied onto the mucosal surface of each of these chosen spots at the different settings previously reported (Fig. 1). After ablation, a second endomicroscopy analysis was performed on the ablated areas, in order to draw a comparison between the histopathological results of each specimen and the endomicroscopy analysis.

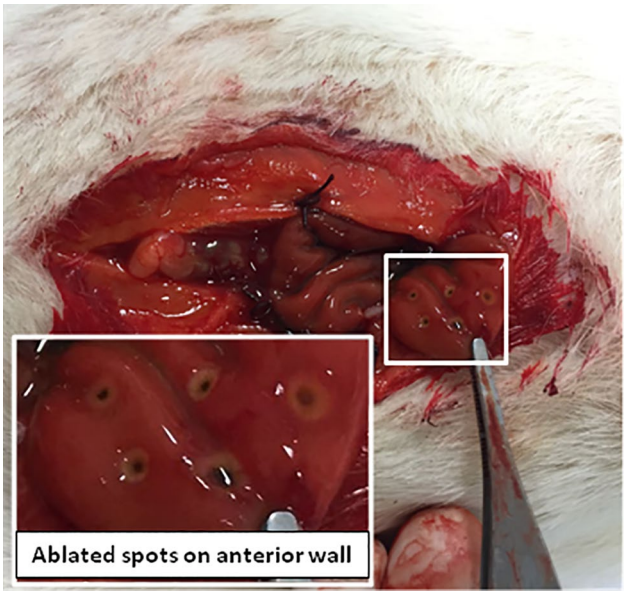

Fig. 1 Experimental setting. Exposure of the gastric wall of the rats. Laser ablation was performed on ten randomly chosen spots. Zoom on the ablation spots

Histopathological analysis

The ablated spots were subsequently excised with at least 0.5 cm of normal tissue for the histopathological analysis. All samples were first fixed in formalin and subsequently embedded in paraffin blocks. Figure 2 shows the details of the histology and of the samples selection. Each sample was cut into 5 µm slices. For each sample, a total of 25 slices were obtained with an interval of 50 µm for every 5 slices selected, with a total of 5250 slices obtained corresponding to a total of 1050 slides prepared (5 slices for each slide). The assumed center of the ablation (evaluated macroscopically) was considered to be the starting point in the first 5-slice sampling. All slides were then stained with hematoxilin and eosin (H&E). The histological analysis to evaluate the ablation damage was made using a light microscope (Zeiss Axiophot). The AxioVision Rel. 4.8 image analysis software was used to acquire pictures of slices at a fivefold enlargement. Only the deepest ablation damage detected for each slide was selected for picture analysis, with a total of 1050 pictures obtained. For each slice, two measurements were taken, i.e., damaged depth (DD) and total depth (TD). Total depth was defined as the sum of mucosal (M) and submucosal (SM) layers (Fig. 2A).

Additionally, in order to assess laser damage severity, an index (DD/*T* ratio) was defined as the ratio between the

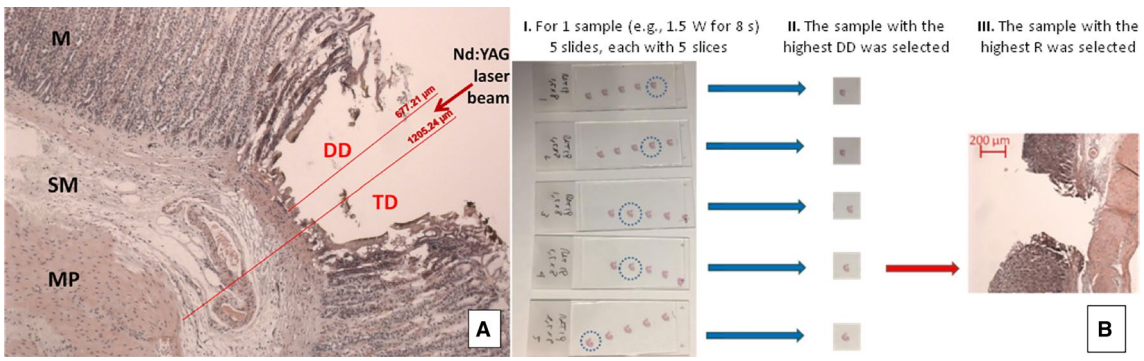

Fig. 2 Histological evaluation of laser ablation. **A** Gastric wall (hematoxilin–eosin; 5×): *DD* damage depth; *TD* total depth, from M to SM. **B** Selection process of the histological slice to include in the study

damage depth over the mucosa and the submucosa thickness, as expressed in Eq. 1:

$$\text{Ratio} = \frac{DD}{TD} = \begin{cases} \text{no damage to } MP, & R \leqslant 1 \\ \text{damage to } MP, & R > 1 \end{cases}. \quad (1)$$

A value of DD/*T* ratio < 1 indicated an ablation damage limited to the *M* or *M* and partial SM (depending on the specific DD/*T* ratio value) without muscularis propria (MP) impairment; DD/*T* ratio = 1 indicated the total ablation of both M and SM without MP impairment; DD/*T* ratio > 1 indicated an ablation involving the MP either partially, or completely.

On histological sections, damage was classified considering the involved layer: complete (*M*) and partial (*M*p) mucosal ablation, complete (SM) and partial (SMp) submucosal ablation, and complete (MP) and partial (MPp) muscularis propria ablation.

In order to evaluate the maximum DD of laser light into the gastric wall for each sample, only the measurement related to the slice with the higher DD/*T* ratio was included. Consequently, the section with the highest DD was selected while it was noted that TD did not vary significantly among the five sections (Fig. 2B). As a result, for each laser setting, the mean values of DD/T ratio were calculated and used to perform the statistical analysis (i.e., for *P* = 2.5 W applied for 12 s, a total of 6 DD/*T* ratio values were obtained. The mean value of these 6 Rs was calculated and used for analysis).

Data analysis

Continuous variables were reported as mean ± standard deviation (SD) and categorical variables as numbers and percentages unless specified otherwise. Ordinal qualitative variables and quantitative variables were compared with a Wilcoxon rank-sum test. A paired comparison of qualitative variables was performed with a Fisher's exact test or Chi-square tests. Correlations between laser settings and DD/T ratio were performed using a Pearson correlation coefficient (Pearson's *r*). A regression analysis was performed with the linear regression method if a correlation was found. All reported *p* values are two-tailed, and a *p* value < 0.05 was required to conclude statistical significance. SPSS software, version 20.0 (IBM-SPSS, Chicago IL), was used for the analysis.

Numerical modeling

Laser–tissue interactions lead to a temperature increase in the target and in the surrounding area [21]. In the field of thermal ablation therapies, numerical models are often used to simulate the heating in the target, at different therapy settings (e.g., power and delivery time). The simulations allow better understanding the potential thermal damage induced by the source, and also transferring the same therapeutic framework to different tissues and models. This last step can be performed by changing both the geometry of the target organ, and its physical properties, which describe the behavior of the tissue with respect to the energy source. In this study, a numerical model was built to simulate the potential thermal outcome of Nd:YAG laser on the human gastric wall. The simulations included blood perfusion and metabolic activities, and the different human gastric layers have been characterized by corresponding optical absorption properties [21]. The numerical model relies on the description of the laser–tissue interaction and on the consequent heat transfer in biological tissues (described by the Pennes' Equation) [22]. The outcome of the numerical model is the temperature distribution resulting in the human gastric wall undergoing laser ablation. The simulations were performed considering power and time settings used for animal experiments and were implemented on the commercial Comsol Multiphysics software.

Results

At both macroscopic and microscopic evaluations, none of the samples reported any full-thickness perforation. The thermal effect involved different layers, with different severities, namely/and notably ablation spread from Mp to complete MP impairment. The different degrees of damage are reported in Fig. 3a.

The relationship between DD/*T* ratio and *E* (J) is well represented using a linear model with a positive trend: an increased damage depth per higher E applications is observed (Fig. 3B). The appropriate agreement between the linear model and the experimental data is confirmed by the high value of the correlation coefficient ($p = 0.0001$; DD/T ratio = 0.838 [CI 95% 0.72–0.89]).

For $E < 4$ J, the mean value of DD/T ratio was always lower than 0.85, subsequently causing only a partial mucosal layer impairment. For $E \geq 15$ J, the mean value of DD/T ratio was higher than 1, leading to an MP impairment. In fact, the higher DD/T ratio value (i.e., 1.33 ± 0.31) was achieved at $E = 30$J.

The best results were obtained for E values comprised between 4 and 12 J, where DD/*T* ratio was higher than 0.9, thereby entailing M and SM ablation.

Mathematical prediction

The predictions provided by the numerical simulation of laser ablation applied to human gastric wall are shown in Fig. 4A. The predictive model of damage depth

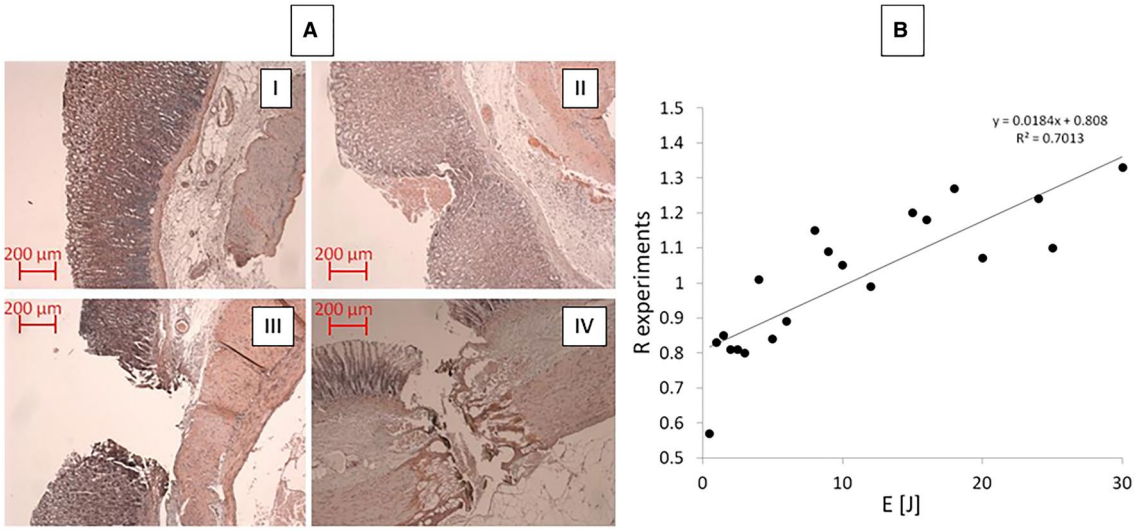

Fig. 3 Histology showing various degrees of laser ablation and correlation with the energy applied. **A** Normal structure (I): partial M ablation (II), M and complete SM ablation (III), and complete ablation of M, SM, and MP (IV). **B** Correlation between mean DD/*T* ratio values and the applied energy (*E* [J]). Experimental data (black dots) and the best fitting line (continuous black line) are shown

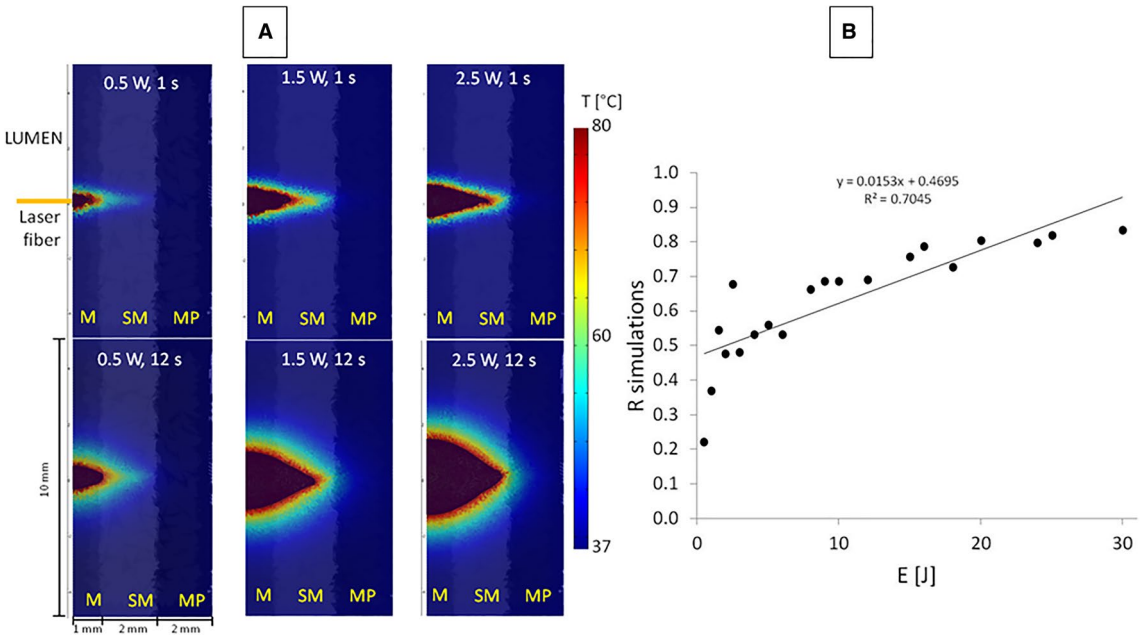

Fig. 4 Numerical predictive model of ablation. **A** Temperature distribution obtained from the numerical simulation on human gastric wall at some *P* (0.5, 1.5, 2.5 W) and *t* (1 and 12 s) settings used for *in vivo* experiments. **B** Correlation between DD/*T* ratio values and the applied energy (*E* [J]). Experimental data (black dots) and the best fitting line (continuous black line) are shown. The theoretical temperature distribution induced by thermal treatment is shown for $P=0.5$, 1.5, and 2.5 W, after 1 and 12 s of ablation. Also in this case, no full-thickness perforation was obtained. The tissue region in contact with the laser applicator experiences complete ablation ($T>80$ °C) for all settings (brown color); nevertheless, the spatial extension of the damage, hence the injured layer, is related to *P* and *t* values. For ablation performed at $P=0.5$ W and $t=1$ s, ablation occurs in M while SM experiences $T<80$ °C, and no dangerous temperature increase is predicted into MP; at $t=12$ s, SM is affected by ablation in the surface only. A more severe SM ablation is predicted for $P=1.5$ and 2.5 W at 1 s, while $t=12$ s also entails a significant temperature increase in the superficial MP layer. However, the ablation is confined to the SM. (Color figure online)

demonstrated a positive linear correlation with *E* settings (Pearson's coefficient = 0.868; 95% CI 0.75–0.98), as shown in Fig. 4B.

The second step consisted in analyzing the correlation between the prediction of the mathematical model and the experimental data.

The predicted DD/*T* ratio data range from 0.22 (for *E* = 0.5 J) to 0.83 (for *E* = 30 J). Figure 5 shows the linear regression between the mean values of the experimental DD/*T* ratio data and the simulated DD/*T* ratio values. The predictive model of damage depth demonstrated a significant positive linear correlation with the experimental data (Pearson's coefficient = 0.85; 95% CI 0.66–0.94).

The endomicroscopy system allowed for a real-time ablation damage assessment. Figure 6 shows the microscopic confocal images acquired before and after treatment at different *P* settings.

Discussion

In this experimental study, we developed and tested a predictive numerical model applied to laser-based ablation of gastrointestinal (GI) lesions. The aim was to develop a model to replicate the mechanical effects of an ESD using a laser source.

Laser-based ablation for the curative treatment of early GI lesions was introduced between the end of the nineteen eighties [23] and the beginning of the nineties [14–18], especially for the treatment of Early Gastric Cancer (EGC), after the successful results obtained in the palliative treatment of advanced GI lesions [24–26]. In a cohort of 111 patients with EGC, Yasuda et al. [18] reported a success rate of 81%. Similarly, Sibille et al. [14] showed an initial complete response in 89% of cases. In addition, at a median follow-up of 33 months, 14 out of 18 patients (77.7%) still reported a complete tumor response. However, the lesions treated were mostly confined in the mucosal layer [14–16, 18]. The application on superficial lesions could well substantiate the low rate of complications reported (2.9%), mainly in terms of bleeding and perforations [15]. On the other hand, the complication rate is much higher when laser ablation is applied to locally advanced GI tumors [27, 28], probably because of a deeper thermal damage induced and/or different tissue properties of infiltrating tumors. The optimal laser settings remain to be determined since there is a large inhomogeneity in terms of power and application time in the published series. Tajiri et al. [15] analyzed the impact of a *P* ranging from 40 to 60 W applied for 0.5 s through a contactless probe, or 15–30 W for 1–2 s through a contact probe, in a cohort of 1158 patients. The authors have reported a 20% recurrence rate at 1 year. Tani et al. [16] applied the Nd:YAG laser with a contactless probe with a 1320 nm wavelength in addition to the conventional 1064 nm wavelength.

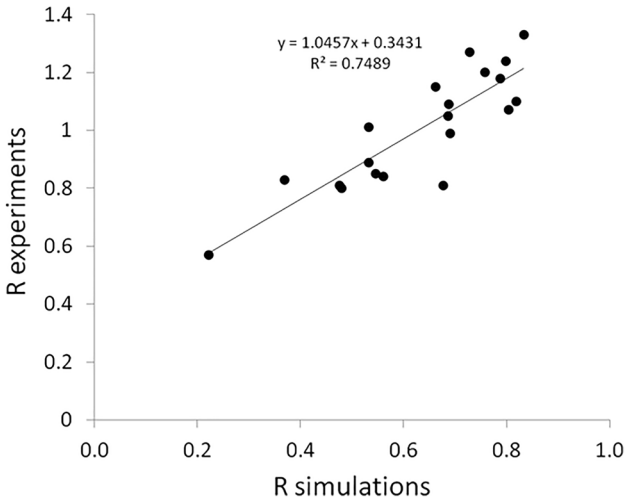

Fig. 5 Correlation between the predicted and experimental values. Correlation between DD/*T* ratio values as predicted by the mathematical model, and experimental DD/*T* ratio values measured at the same *E* settings. Experimental data (black dots) and the best fitting line (continuous black line) are shown

To the best of our knowledge, there were no attempts to consider energy-based ablations as therapeutic strategies for lesions invading the submucosal layer. One of the possible reasons for overlooking this potential application could lie in damage depth unpredictability following the use of the energy source and in the lack of feedback regarding ablation completeness. We previously reported some preliminary experimental data about the possibility to perform a theranostic treatment of GI lesions via the application of endoluminal high-intensity focused ultrasound (HIFU) [8]. In that setting, we took advantage of the HIFU's inability to penetrate through air. A submucosal injection of air could well create a long-lasting lifting and an effective protective cushion. HIFU could yield an effective ablation down to the submucosa and no perforations occurred.

When the energy used is a laser, there is no easy way to block the progression of energy delivery to the tissues and as a result, the possibility to preoperatively obtain adequate P and t settings would lead to an optimized ablation therapy, potentially for both mucosal and submucosal infiltrating lesions. This approach might extend the principle of energy-based removal at submucosal level, while sparing the muscularis propria layer. This study was mainly aimed to find the P and t application settings suitable to induce the desired ablation. Since thermal damage increases with applied energy settings, safe M and SM ablations were achieved applying *E* between 4 and 12 J while higher values are related to a more frequent MP impairment.

The mathematical model described the thermal outcome induced by laser ablation onto human gastric wall.

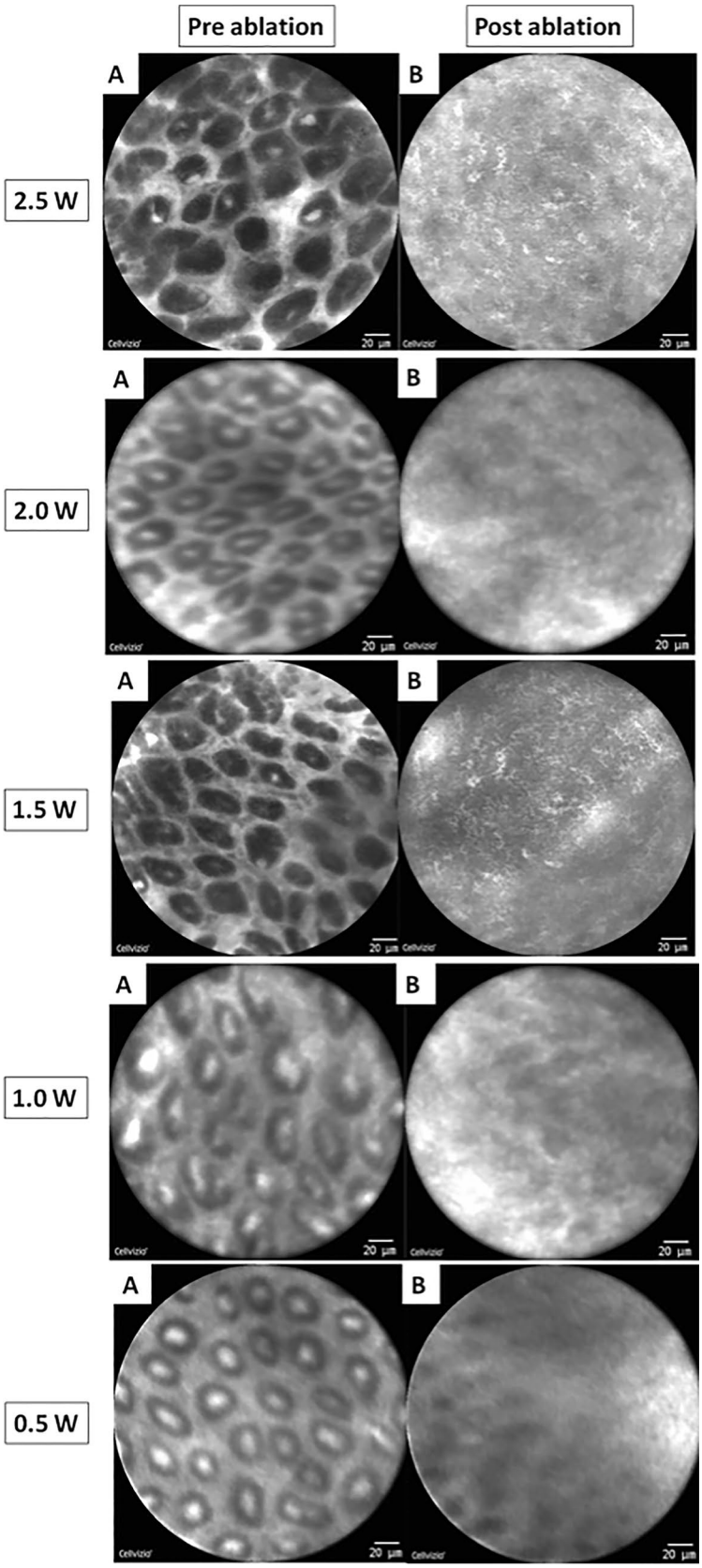

Fig. 6 Confocal images acquired before (**A**) and after (**B**) laser ablation. In all cases, before ablation, a regular shape of gastric cells was observed (**A**) while a distortion of the architecture and the disappearance of the gland contours occurred in case of thermal damage, with some phantom images of round gastric cells, mainly in case of $P = 0.5$ and 1.0 W. A complete anatomical structure loss was observed when ablation was performed at $P = 1.5$, 2.0, and 2.5 W (**B**)

This model allowed to take into account the larger thickness of the human gastric layers with respect to the rodents and also to consider the optical absorption properties of the human gastric wall by using data provided by the literature [21]. The same laser settings tested on the rodents have been implemented in the simulations, aiming to predict the thermal effects of those setting in a potential human case. $P = 0.5$ W caused the ablation of MM only after a 1 s treatment and extends to SM for higher t values. In other words, when theoretically applied to human stomach gastric tissue, the thermal damage was always confined to the SM in all the simulated cases ($P = 1.5$–2.5 W at different t values).

Care should be taken when applying a higher E value, i.e., 30J (2.5 W for 12 s). Indeed, although the ablation seems to remain confined to M and SM layers, a significant temperature increase (about 60 °C) could occur at the surface of the MP layer. A temperature around 60 °C is potentially dangerous since it can induce irreversible thermal damage, even if it generally does not induce tissue vaporization [22].

Simulations are obtained considering the properties of the normal gastric wall, and different results could probably be observed when considering tumor tissue. Tumor tissue properties are expected to be different, inducing a potential different spread of the thermal damage. Further studies are already planned on the application of this same ablative technique on animal bearing early GI tumors. The preliminary results of this experimental study represent a step toward the possibility to select the optimal laser setting for a safe and controlled ablative treatment of GI lesions.

Confocal laser endomicroscopy (CLE) is a technology providing magnified, high-resolution, real-time, in vivo virtual biopsies of tissues [29–32]. Images are obtained upon the administration of a contrast agent and by scanning of the tissue with low-power laser light. The light–tissues interactions are captured and analyzed to reconstruct the images. Our hypothesis was that CLE could identify the thermal damage and was used in this experimental work as a complementary tool to the conventional histopathological analysis.

CLE could detect significant differences in terms of tissue architecture before and after ablation. In addition, differences were also noted in case of different Ps applied. As an example, for $P = 0.5$ W, a gradual passage was noted between ablated and normal tissue, with the presence of "phantom cells" between the two areas. Conversely, in case of a higher P, a prompter delineation was observed between ablated and non-ablated zones.

In the framework of laser application to early GI tumors, the endomicroscopy system, particularly if coupled with the use of fluorescein-labeled cancer-specific antibodies [33], would be useful in the evaluation of residual tumor cells after laser ablation, assisting in the real-time decision-making process when it comes to further applications. In fact, there is an emerging field defined as molecular fluorescence-guided surgery which could provide an optical signature of complete ablation [34]. In this paradigm, targeted fluorophores made of monoclonal antibodies combined with fluorescent molecules can selectively highlight tumor tissue. The variation occurring with the fluorescent signal after laser treatment could provide information on the radicality of the ablation. In other terms, the reduction or the disappearing of the fluorescence signal upon laser ablation of the tumor area might be a marker of response to the local treatment. At our institute of image-guided surgery, a dedicated research unit was created to develop molecular fluorescence-guided treatments (IHU-SPECTRA, Integrated HUb for shining perioperative endoscopic theranostics). A large research project (ELIOS), funded by the French Research Foundation against Cancer (ARC Foundation), is underway to test diagnostic properties of targeted fluorophores in the clinical setting. Additionally, comparative studies between different forms of energy to achieve endoscopic submucosal ablations, including laser, HIFU, and RF, are planned, in the large animal model.

Conclusion

Low-power laser settings achieved an effective and safe mucosal and submucosal ablation. The numerical model developed helped to accurately predict the ablated layers. Confocal endomicroscopy provided a real-time visualization of thermal damage. Further studies geared to test the selected settings in a large animal model (e.g., swine) and in a rodent model with early GI tumors will lead to the definition of the appropriate modality for potential clinical applications.

Acknowledgements Authors would like to thank Christopher Burel and Guy Temporal, professionals in Medical English proofreading, for their valuable help in revising the manuscript.

Funding This study was partly funded by the ARC Foundation, through the ELIOS Grant (PI: Michele Diana).

Compliance with ethical standards

Disclosures Michele Diana is the recipient of a grant from the ARC Foundation. Jacques Marescaux is the President of IRCAD and IHU-Strasbourg institutes, which are partly funded by Karl Storz, Siemens Healthcare, and Medtronic. Drs. Giuseppe Quero, Paola Saccomandi, Jung-Myun Kwak, Bernard Dallemagne, Guido Costamagna, Didier Mutter, have no conflicts of interests or financial ties to disclose.

References

1. Marin-Gabriel JC, Fernandez-Esparrach G, Diaz-Tasende J, Herreros de Tejada A (2016) Colorectal endoscopic submucosal

dissection from a Western perspective: today's promises and future challenges. World J Gastrointest Endosc 8:40–55
2. Holmes I, Friedland S (2016) Endoscopic mucosal resection versus endoscopic submucosal dissection for large polyps: a Western colonoscopist's view. Clin Endosc 49:454–456
3. Uedo N, Takeuchi Y, Ishihara R (2012) Endoscopic management of early gastric cancer: endoscopic mucosal resection or endoscopic submucosal dissection: data from a Japanese high-volume center and literature review. Ann Gastroenterol 25:281–290
4. Ohta T, Ishihara R, Uedo N, Takeuchi Y, Nagai K, Matsui F, Kawada N, Yamashina T, Kanzaki H, Hanafusa M, Yamamoto S, Hanaoka N, Higashino K, Iishi H (2012) Factors predicting perforation during endoscopic submucosal dissection for gastric cancer. Gastrointest Endosc 75:1159–1165
5. Oda I, Suzuki H, Nonaka S, Yoshinaga S (2013) Complications of gastric endoscopic submucosal dissection. Dig Endosc 25(Suppl 1):71–78
6. Hanaoka N, Uedo N, Ishihara R, Higashino K, Takeuchi Y, Inoue T, Chatani R, Hanafusa M, Tsujii Y, Kanzaki H, Kawada N, Iishi H, Tatsuta M, Tomita Y, Miyashiro I, Yano M (2010) Clinical features and outcomes of delayed perforation after endoscopic submucosal dissection for early gastric cancer. Endoscopy 42:1112–1115
7. Baldaque-Silva F, Cardoso H, Lopes J, Carneiro F, Macedo G (2013) Radiofrequency ablation for the treatment of gastric dysplasia: a pilot experience in three patients. Eur J Gastroenterol Hepatol 25:863–868
8. Diana M, Schiraldi L, Liu YY, Memeo R, Mutter D, Pessaux P, Marescaux J (2016) High intensity focused ultrasound (HIFU) applied to hepato-bilio-pancreatic and the digestive system-current state of the art and future perspectives. Hepatobiliary Surg Nutr 5:329–344
9. Luigiano C, Iabichino G, Eusebi LH, Arena M, Consolo P, Morace C, Opocher E, Mangiavillano B (2016) Outcomes of radiofrequency ablation for dysplastic Barrett's esophagus: a comprehensive review. Gastroenterol Res Pract 2016:4249510
10. Mao Y, Qiu H, Liu Q, Lu Z, Fan K, Huang Y, Yang Y (2013) Endoscopic holmium:YAG laser ablation of early gastrointestinal intramucosal cancer. Lasers Med Sci 28:1505–1509
11. Peter S, Monkemuller K (2015) Ablative endoscopic therapies for Barrett's-esophagus-related neoplasia. Gastroenterol Clin North Am 44:337–353
12. Rabenstein T, May A, Gossner L, Manner H, Pech O, Gunter E, Huijmans J, Vieth M, Stolte M, Ell C (2008) Invisible gastric carcinoma detected by random biopsy: long-term results after photodynamic therapy. Endoscopy 40:899–904
13. Schena E, Saccomandi P, Fong Y (2017) Laser ablation for cancer: past, present and future. J Funct Biomater 8
14. Sibille A, Descamps C, Jonard P, Dive C, Warzee P, Schapira M, Geubel A (1995) Endoscopic Nd:YAG treatment of superficial gastric carcinoma: experience in 18 Western inoperable patients. Gastrointest Endosc 42:340–345
15. Tajiri H, Oguro Y (1991) Laser endoscopic treatment for upper gastrointestinal cancers. J Laparoendosc Surg 1:71–78
16. Tani M, Takeshita K, Honda T, Saito N, Endo M (1997) Results of endoscopic treatment for early gastric cancer by Nd-YAG Laser. Diagn Ther Endosc 3:203–210
17. Yang GR, Zhao LQ, Li SS, Qiu SL, Wang YM, Jia JH (1994) Endoscopic Nd:YAG laser therapy in patients with early superficial carcinoma of the esophagus and the gastric cardia. Endoscopy 26:681–685
18. Yasuda K, Mizuma Y, Nakajima M, Kawai K (1993) Endoscopic laser treatment for early gastric cancer. Endoscopy 25:451–454
19. Lightdale CJ, Heier SK, Marcon NE, McCaughan JS Jr, Gerdes H, Overholt BF, Sivak MV Jr, Stiegmann GV, Nava HR (1995) Photodynamic therapy with porfimer sodium versus thermal ablation therapy with Nd:YAG laser for palliation of esophageal cancer: a multicenter randomized trial. Gastrointest Endosc 42:507–512
20. Saccomandi P, Quero G, Costamagna G, Diana M, Marescaux J (2017) Effects of Nd:YAG laser for the controlled and localized treatment of early gastrointestinal tumors: Preliminary in vivo study. Conf Proc IEEE Eng Med Biol Soc 2017:4533–4536
21. Müller GJ, Roggan A (1995) Laser-induced interstitial thermotherapy. SPIE Press, Bellingham
22. Saccomandi P, Schena E, Caponero MA, Di Matteo FM, Martino M, Pandolfi M, Silvestri S (2012) Theoretical analysis and experimental evaluation of laser-induced interstitial thermotherapy in ex vivo porcine pancreas. IEEE Trans Biomed Eng 59:2958–2964
23. Takemoto T (1986) Laser therapy of early gastric carcinoma. Endoscopy 18(Suppl 1):32–36
24. Fleischer D, Kessler F, Haye O (1982) Endoscopic Nd: YAG laser therapy for carcinoma of the esophagus: a new palliative approach. Am J Surg 143:280–283
25. Fleischer D, Sivak MV Jr (1985) Endoscopic Nd:YAG laser therapy as palliation for esophagogastric cancer. Parameters affecting initial outcome. Gastroenterology 89:827–831
26. Tytgat GN (1990) Endoscopic therapy of esophageal cancer: possibilities and limitations. Endoscopy 22:263–267
27. Mellow MH, Pinkas H (1984) Endoscopic therapy for esophageal carcinoma with Nd:YAG laser: prospective evaluation of efficacy, complications, and survival. Gastrointest Endosc 30:334–339
28. Naveau S, Chiesa A, Poynard T, Chaput JC (1990) Endoscopic Nd-YAG laser therapy as palliative treatment for esophageal and cardial cancer. Parameters affecting long-term outcome. Dig Dis Sci 35:294–301
29. Diana M, Noll E, Charles AL, Diemunsch P, Geny B, Liu YY, Marchegiani F, Schiraldi L, Agnus V, Lindner V, Swanstrom L, Dallemagne B, Marescaux J (2017) Precision real-time evaluation of bowel perfusion: accuracy of confocal endomicroscopy assessment of stoma in a controlled hemorrhagic shock model. Surg Endosc 31:680–691
30. Wu T, Heuillard E, Lindner V, Bou About G, Ignat M, Dillenseger JP, Anton N, Dalimier E, Gosse F, Foure G, Blindauer F, Giraudeau C, El-Saghire H, Bouhadjar M, Calligaro C, Sorg T, Choquet P, Vandamme T, Ferrand C, Marescaux J, Baumert TF, Diana M, Pessaux P, Robinet E (2016) Multimodal imaging of a humanized orthotopic model of hepatocellular carcinoma in immunodeficient mice. Sci Rep 6:35230
31. Diana M, Robinet E, Liu YY, Legner A, Kong SH, Schiraldi L, Marchegiani F, Halvax P, Swanstrom L, Dallemagne B, Marescaux J (2016) Confocal imaging and tissue-specific fluorescent probes for real-time in vivo immunohistochemistry. Proof of the concept in a gastric lymph node metastasis model. Ann Surg Oncol 23:567–573
32. Diana M, Dallemagne B, Chung H, Nagao Y, Halvax P, Agnus V, Soler L, Lindner V, Demartines N, Diemunsch P, Geny B, Swanstrom L, Marescaux J (2014) Probe-based confocal laser endomicroscopy and fluorescence-based enhanced reality for real-time assessment of intestinal microcirculation in a porcine model of sigmoid ischemia. Surg Endosc 28:3224–3233
33. Englhard AS, Palaras A, Volgger V, Stepp H, Mack B, Libl D, Gires O, Betz CS (2017) Confocal laser endomicroscopy in head and neck malignancies using FITC-labelled EpCAM- and EGFR-antibodies in cell lines and tumor biopsies. J Biophotonics 10:1365–1376
34. Harlaar NJ, Koller M, de Jongh SJ, van Leeuwen BL, Hemmer PH, Kruijff S, van Ginkel RJ, Been LB, de Jong JS, Kats-Ugurlu G, Linssen MD, Jorritsma-Smit A, van Oosten M, Nagengast WB, Ntziachristos V, van Dam GM (2016) Molecular fluorescence-guided surgery of peritoneal carcinomatosis of colorectal origin: a single-centre feasibility study. Lancet Gastroenterol Hepatol 1:283–290